Dynamics of nucleation in binary alloys

Thomas Philippe

Article

Dynamics of Nucleation in Binary Alloys

Thomas PHILIPPE*
Laboratoire de Physique de la Matière Condensée, CNRS, Ecole polytechnique, Institut Polytechnique de Paris, 91120 Palaiseau, France
*thomas.philippe1984@gmail.com

Abstract

Nucleation in binary alloys is studied in the capillary approximation of classical theory. By allowing both the size of the cluster and its composition to vary, the phase transition is investigated in a two-dimensional space. This parametrization allows to derive diffusivities of the Fokker-Planck equation for the distribution function of clusters from the Cahn-Hilliard equation. It is shown how kinetics, together with thermodynamics, determine the direction of the nucleation current as well as the magnitude of the nucleation rate. The properties of the critical clusters and the direction of the nucleation current at the saddle point are derived for a generic model, from the binodal line to the spinodal limit. The critical clusters are found to exhibit properties that are very similar to that of non-classical theories. Once moderate supersaturation is reached, the interplay between kinetics and thermodynamics is found to invalidate the classical picture by modifying the direction of the nucleation current. The consequences on the magnitude of the rate of nucleation are discussed. The model is then applied to decomposition of FeCr solid solutions and is shown to constitute a reasonable sharp-interface approximation of the diffuse-interface theory of nucleation for the determination of both the cluster properties and the nucleation rate.

Key words

nucleation, clusters, direction of flux, rate of nucleation

1. Introduction

Classical nucleation theory (CNT) [1–6] is usually the starting point of any model describing the initial stages of a phase transformation. Thermodynamics of CNT is most often established within the capillary model [7], i.e. the embryo of the new phase is a sphere separated from the mother phase by a sharp interface that gives rise to an energy penalty proportional to the interface area. As opposed to the Gibbs model [8], the interface is not treated as a separate entity but is assumed to belong to the cluster in the capillary approximation. Various refinements have been proposed to improve the original theory [9], one can mention for instance the Tolman correction, employed to account for the curvature effect on surface tension. In the usual application of classical nucleation theory, the embryo is described by its size, or the number of atoms or molecules it contains, and is assumed to present, whatever its size, the properties of the equilibrium phase, in terms of density, composition, order or crystalline structure. Making this assumption and considering the size as the only parameter of the theory is is not appropriate in some cases. This has been evidenced experimentally and in many computational works, for the crystallisation of water, colloids and proteins [10–13], or in crystallisation and precipitation of metallic alloys [14–16], to name just a few examples. One way to relax this assumption is to consider a diffuse interface, as done in the so-called Cahn-Hilliard theory of nucleation [17–21]. Such approaches, also known as square gradient or diffuse interface theories [22, 23], can be seen as the first approximation to density functional theory [24–27]. The latter theories are naturally more accurate than CNT in the determination of the critical cluster properties and in the calculation of the nucleation barrier [9] since the sharp-interface approximation is relaxed. The latter properties, evaluated at the saddle-point of the energy surface, result from thermodynamic considerations. Nevertheless, the quantity of interest is primarily the rate at which clusters overcome the nucleation barrier and enter into the growth regime, given by the so-called nucleation rate. However, a proper calculation of this rate in the framework of diffuse interface theories is non trivial since the energy landscape is highly multidimensional in this case, which makes this problem difficult to solve. To our knowledge, a proper determination of the nucleation rate has been attempted only very recently in the phase-field framework [28, 29], consequently the approach is necessarily numerical.

In this work, we employ a different strategy by using the capillary model but with a treatment of thermodynamics that does not fix the cluster composition and surface energy to equilibrium [7, 30]. We remain in the CNT framework in order to derive an analytical expression of the nucleation rate, the first quantity of interest in any nucleation theory. This thermodynamic treatment was shown to essentially captures the main properties of the diffuse critical nucleus [8, 18, 27, 30–34] and is therefore a good candidate for describing nucleation in the whole binodal domain. This approach has been employed in many different applications of nucleation theory [8, 18, 27, 30–36]. It is known as the generalized Gibbs theory [32] or sometimes as the modified CNT [36] but was first introduced in 1976 by Reiss et al. [30] as merely a more careful thermodynamics treatment of CNT. Therefore, the latter model is not new but its couplings with the Cahn-Hilliard (CH) equation, as

detailed in the following analysis, is original. In this work, we consider nucleation in solids for a binary alloy and allow both the size of the clusters and their composition (atomic fraction) to vary. We neglect elastic contributions, the latter being negligible, at nanoscale, in many alloys [37]. In nucleation theory, parameters used to describe the clusters are known as reaction coordinates [38–45]. Thus, our model presents two reaction coordinates: the cluster size R, and its composition c. The fact that the composition of the cluster may be different from equilibrium, given by the phase diagram, implies that the driving force for nucleation can differ from the classical expression, and the surface energy depart from its equilibrium value. This allows for a thermodynamics treatment closer to non-classical diffuse-interface theories. In this letter, we determine the properties of the critical nucleus but we are particularly interested in the nucleation dynamics, thus, we show how recent theoretical developments [45–47] can be used to derive an explicit formulation of the nucleation rate in the present model. This task is non trivial because one needs to determine the direction of the current, that is, in general, not given by the direction of steepest descent of the saddle surface as the kinetic characteristics of the system may deviate the nucleation current. The nucleation rate results therefore from a complex interplay between thermodynamics and kinetics. Here, we show how kinetics, imposed by the Cahn-Hilliard equation, governs the nucleation rate of first order phase transitions in binary systems.

2. Governing equations

The classical method to study the kinetics of nucleation is based on the Fokker-Planck equation for the distribution function of clusters $f(R,c,t)$ [2, 45]:

$$\frac{\partial f}{\partial t} = -\frac{\partial J_i}{\partial x_i} \tag{1}$$

for $i = R,c$ and $x_i = R,c$ with

$$J_i = -D_{ij}\frac{\partial f}{\partial x_j} + \dot{x}_i f. \tag{2}$$

The first term of the RHS describes diffusion on the energy landscape, the second term is a drift term. Fokker-Planck diffusivities D_{ij} in this space are assumed to be constant and taken at their value near the critical cluster. The Fokker-Planck equation is generally considered in the size space with f a particle-size distribution function in this context (see a textbook description in Ref. [48]) and has been studied in many different works related to nucleation [49–52] and crystal growth [53–55]. In the present study, nucleation is investigated in a two-dimensional space of size R and composition c where f is therefore the distribution function of clusters of size R and composition c at time t. Note that the above equations are written in their dimensionless form, with $\tilde{R} = Rb^{-1/3}$ with b an atomic volume. f has also been scaled by b^{-1} and is therefore dimensionless, as for the fluxes. c is a rescaled composition, $c = \nu\left(c' - c'_c\right)$, where c' is the atomic fraction, ν and c'_c are parameters of the thermodynamic model, that we will explicit later. Time has been scaled by $\tau = b^{5/3}/\left(\nu^2 MkT\right)$ with M the traditional mobility employed in the CH equation (in

$m^5J^{-1}s^{-1}$). Tildes are then omitted for sake of clarity and Einstein's notations are used for sake of conciseness. The work of formation $\Delta\Omega$, scaled by kT, determines the equilibrium distribution corresponding to heterophase fluctuations:

$$f_0 = Ce^{-\Delta\Omega}. \tag{3}$$

with C a dimensionless normalization constant. $\Delta\Omega$ is expanded around the saddle point of the energy surface $\Delta\Omega^*$:

$$\Delta\Omega = \Delta\Omega^* + \frac{1}{2}H_{ij}\left(x_i - x_i^*\right)\left(x_j - x_j^*\right) \tag{4}$$

where $H_{ij} = \frac{\partial^2\Delta\Omega}{\partial x_i \partial x_j}$ at the saddle point with, as before, $i = R, c$ and $x_i = R, c$. R^* and c^* denote the values at the saddle point. For this f_0 we have $J_i = 0$ as the drift and diffusion terms compensate, one finds

$$\dot{x_i} = -D_{ij}\frac{\partial\Delta\Omega}{\partial x_j} \tag{5}$$

Such drift coefficients maintain the distribution at equilibirum ($J_i = 0$) despite f_0 is not homogeneous in the (R, c)-space. Using the above result, one obtains for the fluxes

$$J_i = -D_{ij}\left(\frac{\partial f}{\partial x_j} + f\frac{\partial\Delta\Omega}{\partial x_j}\right), \tag{6}$$

which is also the form used by Langer [56, 57] in the so-called statistical theory of the decay of metastable states. As Alekseechkin [45] we introduce the $\mathbf{Z}$ matrix as follows

$$\dot{x_i} = -D_{ij}\frac{\partial\Delta\Omega}{\partial x_j} = -D_{ij}H_{jk}\left(x_k - x_k^*\right) = -Z_{ik}\left(x_k - x_k^*\right), \tag{7}$$

thus, $\mathbf{Z} = \mathbf{DH}$. Once this matrix is known, the nucleation rate I, at steady state, can be calculated as [45]:

$$I = C\left(2\pi\right)^{\frac{p-2}{2}}\frac{|\lambda|}{\sqrt{|\det\mathbf{H}|}}e^{-\Delta\Omega^*}. \tag{8}$$

with λ the negative eigenvalue of the matrix $\mathbf{Z}$. p is the dimensionality of the space under consideration, $p = 2$ in the (R, c)-space. Note that the above result is dimensionless, $I\left(b\tau\right)^{-1}$ is the practical rate (in unit volume and unit of time). One shall also notice that the normalization constant C depends on the considered space. The above result for the nucleation rate derived by Alekseechkin [45] coincides with the previous expression of the nucleation rate proposed by Trinkaus in his seminal paper [41], which was a more explicit formulation of Stauffer's result [39]. It is also identical to the classical result obtained by Langer [56]. In order to evaluate the nucleation rate, as given by Eq.8, we first need to derive $\mathbf{Z}$ to calculate the eigenvalue. The $\mathbf{Z}$ matrix results from a complex interplay between thermodynamics and kinetics. Indeed, one needs a thermodynamic model to evaluate the

work of formation $\Delta\Omega^*$ and then $\mathbf{H}$, as well as kinetic information to compute the matrix $\mathbf{D}$. The latter may sometimes be obtained directly from microscopic considerations. However, the direct calculation of $\mathbf{D}$ is impossible in some cases when, for instance, the local environment around the nucleus needs to be considered [52]. At this stage, one has to specify a model for the thermodynamics of the system, to compute $\mathbf{H}$, and a dynamic model. For the latter, we start with the usual Cahn-Hilliard equation for the time evolution of a composition profile $c_p(\vec{r})$, here in its dimensionless form:

$$\frac{\partial c_p(\vec{r})}{\partial t} = \nabla^2 \mu(\vec{r}) \tag{9}$$

with $\mu(\vec{r}) = b\frac{\delta\Delta\Omega}{\delta c_p(\vec{r})}$. For spherical clusters, the radial composition profile $c_p(r)$ needs to satisfy the following boundary conditions $\partial c_p(r)/\partial r = 0$ in $r = 0$ and $r \to \infty$ and $c_p(r) = c_0$, the initial composition, in $r \to \infty$. We then employ the method proposed by Lutsko [46, 47]. It relies on a parametrization of the density profile in order to derive from the Cahn-Hilliard equation a dynamical equation for R and a separate one for c, the two parameters of our nucleation theory. The detailed procedure can be found in Refs.[46, 47] in the framework of the dynamical density functional theory. The latter calculation is applied to the Cahn-Hilliard equation in the present analysis and is briefly reproduced in the following. This will allow us to derive the matrix $\mathbf{Z}$ imposed by the CH dynamics and therefore λ. The simplest parametrization is that considered in CNT, inside the cluster the composition is uniform (and equal to c, or c^* at the saddle point), outside the matrix composition is also uniform and is equal to c_0, that of the initial phase, i.e. $c_p(r) = c$ for $r < R$ and $c_p(r) = c_0$ otherwise. We first introduce the quantity $n(r)$ in the sphere of radius r as follows

$$n(r) = \int_{r'<r} c_p\left(\vec{r}'\right) d\vec{r}'. \tag{10}$$

We then integrate the dynamical equation (Eq.9) and use Gauss' theorem to convert the integral to a surface integral, one obtains:

$$\frac{1}{4\pi r^2}\frac{\partial n(r)}{\partial t} = \frac{\partial \mu(\vec{r})}{\partial r}. \tag{11}$$

Multiplying by $\partial n/\partial R$ and integrating one more time leads, for the parameterized $n(r) = n(r,R,c)$, to the following set of equations

$$\dot{x}_i = -g_{ij}^{-1} H_{jk}(x_k - x_k^*) \tag{12}$$

with $i = R, c$ and $x_i = R, c$. The g_{ij}^{-1} are the coefficient of the inverse matrix of $\mathbf{g}$, given by [47]

$$g_{ij} = \int_0^\infty \frac{1}{4\pi r^2}\frac{\partial n(r)}{\partial x_i}\frac{\partial n(r)}{\partial x_j} dr. \tag{13}$$

Eq.12 is an approximated result for any finite parametrization of the concentration profile. In the current model two parameters (R, c) are used to describe the nucleus, where c is the

uniform composition of a cluster of size R separated from the matrix by a sharp-interface. This implies $n = 4\pi r^3 c/3$ for $r < R$ and $n = 4\pi R^3 c/3 + 4\pi \left(r^3 - R^3\right) c_0/3$ otherwise. A more sophisticated parametrization shall result in a more realistic description of the dynamics [35, 47, 58, 59]. Nevertheless, our description is consistent with CNT and we expect it to be valid in the very first stages of growth and therefore appropriate for the calculation of the nucleation rate. The $\mathbf{g}$ matrix is thus evaluated from Eq.13 at the saddle point, in $R = R^*$ and $c = c^*$. Comparing Eq.12 to Eq.7 necessarily implies $\mathbf{Z} = \mathbf{g}^{-1}\mathbf{H}$, i.e. $\mathbf{g}^{-1} = \mathbf{D}$. This is one of the main results of this letter, allowing us to derive the nucleation rate (Eq.8) from the macroscopic CH equation.

In the traditional application of CNT, when only the size of cluster is considered, applying Eq. 8 gives for the nucleation rate

$$I = C g_{RR}^{-1} \sqrt{\frac{|H_{RR}|}{2\pi}} e^{-\Delta\Omega^*} \tag{14}$$

where the Zeldovich result is recovered, as it must. In the one-dimensional theory, one has $g_{RR} = 4\pi \left(R_c^*\right)^3 \left(\bar{c} - c_0\right)^2$, with $\bar{c}$ the cluster composition at equilibrium, as given by the phase diagram. R_c^* is the critical radius. Moreover, $H_{RR} = -8\pi\gamma$ [52], where γ is the dimensionless surface tension. Using g_{RR} and H_{RR} in the above equation for the nucleation rate coincides with the result derived in ref.[52] for diffusion-limited nucleation that, as expected, the dynamics of the CH equation also reproduces.

In the (R, c)-space, the first element of $\mathbf{g}$ is unchanged and we find, from Eq.13, for the other elements: $g_{Rc} = g_{cR} = 4\pi \left(R^*\right)^4 \left(c^* - c_0\right)/3$ and $g_{cc} = (8\pi/15) \left(R^*\right)^5$. R^* and c^* are respectively the radius and the composition of the critical cluster in the two-dimensional theory. Now that $\mathbf{g}$ is known, one needs to derive $\mathbf{H}$ so as to calculate $\mathbf{Z}$ and then its eigenvalue λ. For this purpose, one has to determine $\Delta\Omega$, the work associated to the formation of a cluster of size R and composition c. Still in dimensionless units, we write:

$$\Delta\Omega = -\frac{4}{3}\pi R^3 g_n + 4\pi R^2 K \left(c - c_0\right)^2 \tag{15}$$

where the surface energy term is proportional to $\left(c - c_0\right)^2$, as inspired by squared-gradient theories [8, 17, 35, 36]. K is a constant, determined from the surface energy at equilibrium, $K = \gamma/\left(\bar{c} - c_b\right)^2$. In the one-dimensional theory, $c = \bar{c}$ and $\bar{c} - c_0 \approx \bar{c} - c_b$, the classical form of the surface energy is recovered. g_n is the driving force for nucleation, and depends on c. We can now evaluate $\mathbf{H}$. We find $H_{RR} = -8\pi K \left(c^* - c_0\right)^2$, $H_{Rc} = H_{cR} = -8\pi R^* K \left(c^* - c_0\right)$ and $H_{cc} = -4\pi \left(R^*\right)^3 G/3 + 8\pi \left(R^*\right)^2 K$, $G = \partial^2 g_n/\partial c^2$ is evaluated at the saddle point, i.e. for $c = c^*$. Finally we need to provide a thermodynamic model for the free energy density (g) to calculate the driving force for nucleation as $g_n = g\left(c_0\right) + \left(c - c_0\right)\left[\partial g/\partial c\right]_{c_0} - g\left(c\right)$. In the following, we use a generic $g = -A\left(c^2/2 + c^4/4\right)$ for $c = \nu\left(c' - c_c'\right)$, but a more realistic Landau-type or CALPHAD model shall be employed for any quantitative calculations, if intended [28]. This g function mimics a symmetric phase diagram of critical composition c_c' with ν^{-1} the difference between the critical composition and the binodal

limit. A is a dimensionless constant that allows us to control the magnitude of the driving force. The binodal limit is located at the scaled composition $c_b = -1$ and the spinodal at $c_s = -1/\sqrt{3}$. We study the nucleation regime in the whole binodal domain, for the composition of the initial metastable phase c_0 going from c_b to c_s. In nucleation theory, the properties of the critical clusters (R^*, c^*) corresponds to the saddle point of the energy surface, the latter is unstable and satisfies $\partial\Delta\Omega/\partial R = 0$ and $\partial\Delta\Omega/\partial c = 0$ in R^*, c^*. The energy at the saddle point gives the nucleation barrier $\Delta\Omega^*$. One finds that c^* must satisfy

$$(c - c_0)\frac{dg_n}{dc} = 3g_n \tag{16}$$

and is independent on surface energy, $c^* = c_0 + \sqrt{6c_0^2 - 2}$ for our choice of g. The critical radius is given by

$$R^* = \frac{2K(c^* - c_0)^2}{g_n^*} \tag{17}$$

with $g_n^* = g_n(c^*, c_0)$, and the nucleation barrier by

$$\Delta\Omega^* = \frac{4\pi}{3}R^{*2}K(c^* - c_0)^2. \tag{18}$$

3. Results and discussion

We are interested in comparing our results to the classical picture, for which the critical parameters are denoted by R_c^* and $\Delta\Omega_c^*$. As already mentioned, in the classical treatment the composition is set to its equilibrium value $c_c^* = \bar{c} = 1$. In this comparison, we scale the critical composition as follows $(c^* - c_0)/(c_c^* - c_0)$, the critical size is scaled by R_c^* and the nucleation barrier by $\Delta\Omega_c^*$. Results are therefore independent on K and A. The cluster properties are given in Fig.1.

At low supersaturation (c_0 slightly above c_b), the properties of the critical cluster converge to that of classical picture. However, they are found, as expected [8, 18, 27, 30–33] to rapidly differ from the classical results when increasing the degree of metastability of the initial phase, as c_0 increases. The results of diffuse interface theories are recovered when approaching the spinodal line, the size of the critical cluster diverges, its composition decreases and tends toward that of the initial phase. Concomitantly the nucleation barrier vanishes (Fig.1). The latter quantity intervenes in the exponential part of the nucleation rate and has therefore a drastic impact on its magnitude. Then one calculates the negative eigenvalue of the $\mathbf{Z}$ matrix. In the considered (R, c)-space, one finds

$$\mathbf{Z} = \frac{2K}{R^{*3}}\mathbf{Z}' \tag{19}$$

with $Z'_{RR} = 9$, $Z'_{Rc} = -3R^*\left[7 - 5X(c^* - c_0)^2\right]/(c^* - c_0)$, $Z'_{cR} = -30(c^* - c_0)/R^*$ and $Z'_{cc} = 60 - 45X(c^* - c_0)^2$. $X = \frac{G}{3g_n^*}$. Interestingly, one remarks that the eigenvalue of $\mathbf{Z}'$

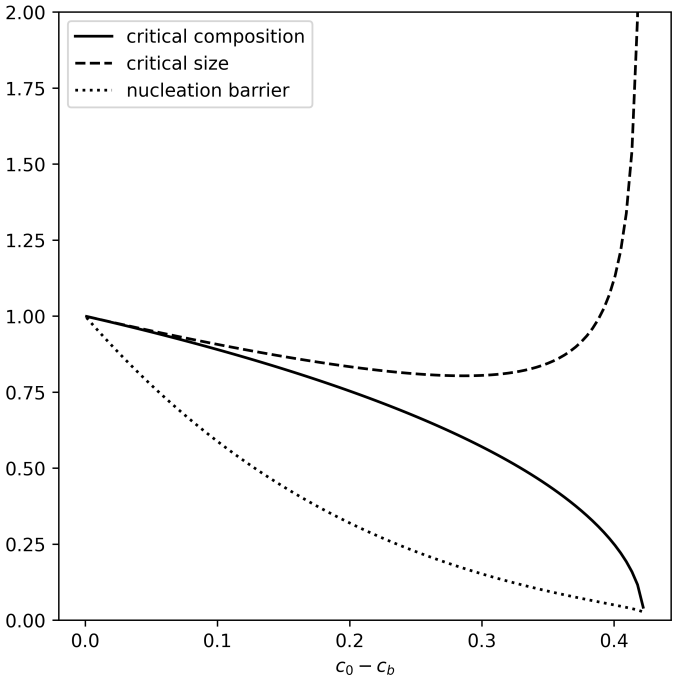

Fig. 1. Properties of the critical clusters compared to the classical picture: R^*/R_c^*, $(c^* - c_0)/(c_c^* - c_0)$ and $\Delta\Omega^*/\Delta\Omega_c^*$ as a function of the initial phase composition in the whole binodal domain.

tends to -1 when c_0 approaches the binodal limit, in this case $\lambda \to -2K/R^{*3}$, which is the value of the classical theory λ_c, calculated as H_{RR}/g_{RR}. The main advantage of the present model is that we arrive at a fully analytical expression for both $\mathbf{Z}'$ and its eigenvalue λ':

$$\lambda' = \frac{Z'_{RR} + Z'_{cc} - \sqrt{\Delta'}}{2} \tag{20}$$

with $\Delta' = (Z'_{RR} - Z'_{cc})^2 + 4Z'_{Rc}Z'_{cR}$. λ' only depends on $X(c^* - c_0)^2$ and is found to decrease with supersaturation.

Figure 2 shows the eigenvalues λ of the present model , i.e. in the two-dimensional space of size R and composition c, as a function of c_0 (for $K = 0.15$ and A=1). For comparison, the values corresponding to the classical treatment are also reported, λ_c, when the size if the only parameter of the theory. λ is found to significantly depart from λ_c once moderate supersaturation is reached. It reaches a maximum and then decreases when approaching the spinodal domain. A similar behavior has been recently evidenced in diffuse interface theories [29]. The fact that the eigenvalue departs from λ_c at high supersaturation suggests that nucleation differs from the classical picture. In classical theory, the cluster size is the unstable variable and evolves as $R(t) \sim \exp(|\lambda_c| t)$ in the overcritical region, according to Eq.7. Any departure from λ_c implies that R is no more the unstable coordinate. In order to understand this effect, one has to determine the direction of the nucleation

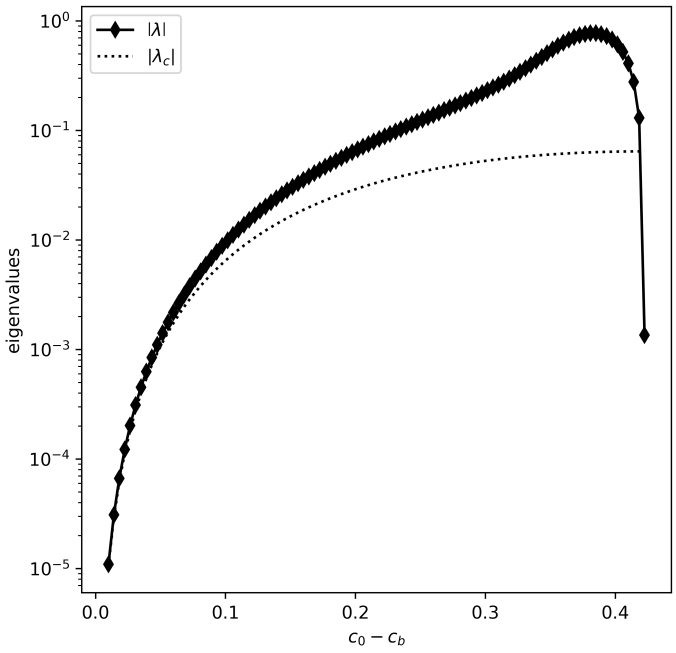

Fig. 2. Eigenvalue $|\lambda|$ and its classical value $|\lambda_c|$ as a function of the initial phase composition. λ is calculated in the two-dimensional space of size R and composition c and λ_c corresponds to the usual one-dimensional version of CNT, i.e. the only parameter is the size and the cluster composition is set to its equilibrium value.

current. Once the matrix $\mathbf{Z}$ is known, one can show that the flux is lying on the line of direction θ calculated as [45]

$$\tan\theta = \frac{\lambda' - Z'_{RR}}{Z'_{Rc}}. \tag{21}$$

λ' only depends on $X\left(c^* - c_0\right)^2$ and Z'_{RR} is constant. Z'_{Rc} also depends on $X\left(c^* - c_0\right)^2$ and increases with R^*. In the present model, the latter is proportional to $d = K/A$ at fixed supersaturation. Therefore, as d increases, the nucleation current progressively aligns with the R-axis, up to $c_0 - c_b \sim 0.32$ for which $Z'_{Rc} = 0$, i.e. $7 - 5X\left(c^* - c_0\right)^2 = 0$. At this supersaturation, the nucleation current is necessarily aligned with the composition axis ($\theta \to \pi/2$), which becomes the unstable variable of the nucleation process, contrary to the classical picture. Above this limit, $\theta < 0$ and the direction of nucleation current is given by $\theta + \pi$. The direction of the flux is reported on Fig.3. We observe that the direction of the flux remains parallel to the R-axis at low supersaturation ($\theta \approx 0$). At $c_0 - c_b \sim 0.32$, $\theta \to \pi/2$ and the composition is found to play the role of the unstable variable, revealing a rapid enrichment of the critical cluster with no change in size. Interestingly, for low d values, the direction of the nucleation current is found to rapidly deviates from that of the classical picture, i.e. $\theta = 0$ and R is the unstable variable. Figure 4 shows the energy surface $\Delta\Omega(R,c)$ for $c_0 - c_b = 0.3$, $K = 0.15$ and $A = 1$. First of all, one remarks that the flux direction significantly departs from the steepest descent direction, evidencing the interplay

between thermodynamics and kinetics. Moreover, the critical cluster are dilute (poor in solute) and, according to the direction of the nucleation current, will experience concomitant growth in size and enrichment. This enrichment process can even result in a reduction of size at high supersaturation (Fig.3). Near the spinodal limit the flux direction (approaching π) makes the cluster shrinks with little change in composition. This is counter-intuitive, but the flux direction describes the very first stages of deterministic growth. Once the nucleation barrier is overcome, the dynamics is expected to rapidly make supercritical clusters both enrich and grow.

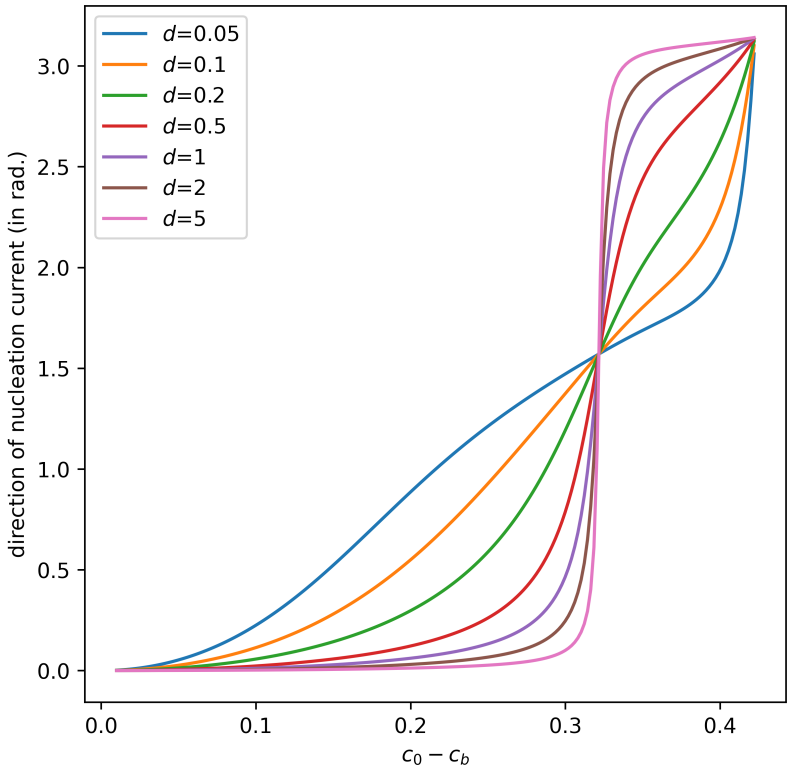

Fig. 3. Direction of the nucleation current as a function of the initial composition, for various $d = K/A$ values.

We find various plausible nucleation pathways near the saddle-point: first the classical regime is recovered near the binodal limit, the cluster grows with the equilibrium composition. Then an intermediate regime can be seen when supersaturation increases, during which a change in size and composition occurs simultaneously. At a given supersaturation value ($Z'_{Rc} = 0$), composition becomes the unstable reaction rate, the cluster enriches with no change in size. The specific value of c_0 depends on the driving force g_n and is therefore model dependent. For our generic choice of g, the transition occurs at relatively high supersaturation. Any classical double-well function is expected to lead to a similar behavior. Finally when approaching the spinodal limit, the cluster shrinks in size with a composition

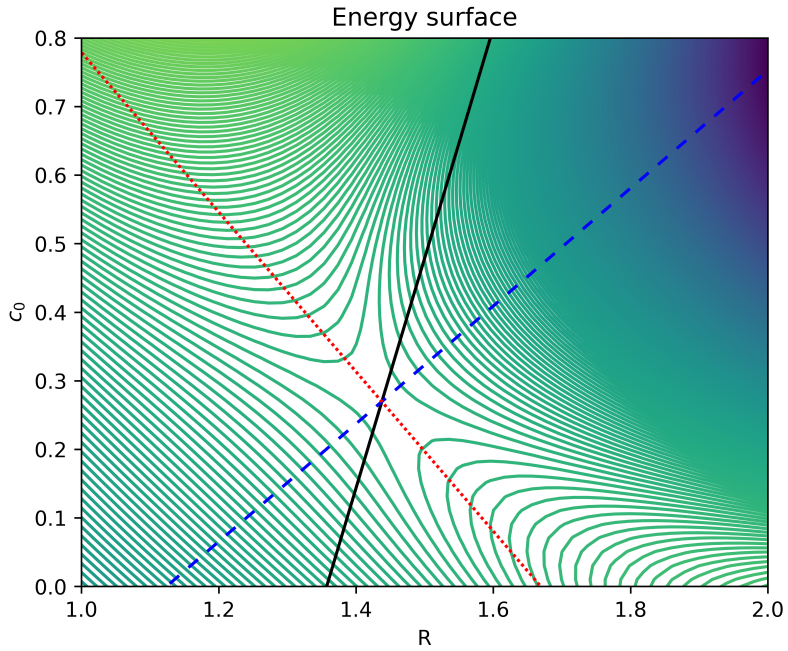

Fig. 4. A contour plot of the energy surface $\Delta\Omega$ for $c_0 - c_b = 0.3$. The direction of the flux (black line), as well as that of steepest descent at the saddle-point (dashed blue line), are shown. The saddle point is located at $(R^*, c^*) = (1.44, 0.27)$. The basin of metastable states is located on the left of the red dashed line.

that is close to that of the initial phase. One needs to mention that those scenario correspond to saddle-point nucleation. Near the spinodal line, the nucleation barrier vanishes and thermal fluctuations are expected to favor ridge-crossing. Nevertheless, the interplay between kinetics and thermodynamics is found to invalidate the classical picture at moderate supersaturation. Once the direction of the nucleation current and the eigenvalue are determined, it remains to calculate the normalization constant to evaluate the nucleation rate with Eq.8. It can be in principle determined from the condition of statistical equilibrium, as in classical theory [45], but we employ a different approach and determine this constant from mass conservation, as follows:

$$\int_{V_m} \frac{4\pi R^3}{3} c' f_0 dc dR = c_0'. \tag{22}$$

The integration is performed over the metastable states (V_m), approximated as the region on the left side of the stable direction at the saddle-point (see Fig.4). Figure 5 shows the dimensionless nucleation rate, still for $A = 1$, $K = 0.15$ and we use, arbitrarily, $\nu^{-1} = 0.353$ and $c_c' = 0.5$ to reproduce the α/α' FeCr phase diagram at 773K [28]. For sake of comparison the classical rate is also reported. The nucleation rate of the present theory is found orders of magnitude larger than the classical result, primarily as the nucleation barrier is lower but also due to the eigenvalue departure from its classical value. The nucleation

rate is also found to exhibit a maximum at high supersaturation, near the spinodal limit, as recently evidenced in the diffuse-interface nucleation theory [29]. An effect that our model also captures.

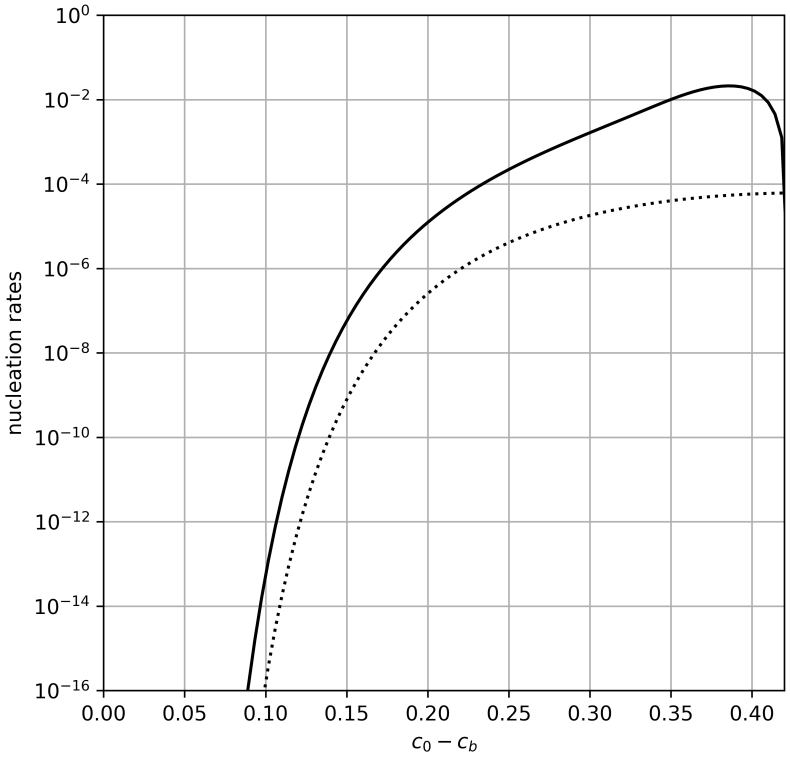

Fig. 5. Dimensionless nucleation rates, in dotted line the classical rate, the solid line corresponds to rate of the present theory.

We conclude this article by applying the model to decomposition of FeCr solid solutions [15, 60]. The "c^2-c^4" free energy density, as well as CALPHAD models [61, 62], are not suitable for quantitative calculations in the FeCr system since they both overestimate the spinodal limit, predicted by thermodynamics databases to be near 0.3 at 773K. Atom probe tomography experiments show that the latter is, in fact, below 25 at.% of Cr [63]. In the diffuse-interface theory developed by Lunéville et al. [28, 29, 37], a "c^6" term was added to the Landau free energy and the coefficients were adjusted to reproduce both the binodal and the spinodal limits at 773K. The same free energy density is employed in our model. In terms of the rescaled composition $c = \nu\,(c' - c'_c)$, the free energy reads $a_2c^2/2 + a_4c^4/4 + a_6c^6/6$ with $a_2 = -0.0035$, $a_4 = -0.654$ and $a_6 = 0.665$, with again $\nu^{-1} = 0.353$ and $c'_c = 0.5$. For the surface energy we use the value given in refs.[28, 29], 0.55 eV/nm^2 i.e. $K = 0.106$ in the present model. The chemical mobility is also needed to calculate the nucleation rate and can be derived from the interdiffusion coefficient in the α phase (D_α), close to 10^{-17} cm^2/s [64]. M is then determined from $D_\alpha = MG_\alpha$ with G_α the Hessian of the free energy density that we evaluate at the equilibirum composition.

The model is applied to a $Fe_{0.81}Cr_{0.19}$ alloy, the critical cluster properties are derived from Eqs.16 and 17, critical clusters are found to contain 44 at.% of Cr and their radius is close to 1 nm, in good agreement with experiments [60] and diffuse-interface predictions [28, 29]. The nucleation barrier is calculated from Eq.18 and is equal to 5.17 k_BT. The nucleation rate is given by Eq.8 and is close to $2\text{x}10^{-8}$ $\text{nm}^{-3}\text{s}^{-1}$, in very good agreement with the rate derived in the diffuse-interface theory [37]. The model is then applied in a $Fe_{0.80}Cr_{0.20}$ alloy. At this initial composition, critical clusters shall contain 40 at.% of Cr and their radius is 0.86 nm. As expected the nucleation barrier is lower and is equal to 1.98 k_BT. The nucleation rate is two order of magnitude larger and is close to $2.4\text{x}10^{-6}$ $\text{nm}^{-3}\text{s}^{-1}$, in very good agreement also with the rate seen in atomistic kinetic Monte Carlo simulations [15, 64]. Classical nucleation is known to fail at predicting both the thermodynamics and kinetics of decomposition of FeCr solid solutions, and of other metallic alloys [16], since it overestimates the nucleation barrier. In this case the diffuse-interface formalism is relevant but rarely used in practice, due to the complexity of its kinetic aspect [29, 56]. The present capillary model, coupled to the Cahn-Hilliard dynamics, is shown to constitute a reasonable sharp-interface approximation of the diffuse-interface theory of nucleation for the determination of both the clusters properties and the nucleation rate.

4. Conclusion

By allowing the composition of clusters to vary in the capillary approximation of classical nucleation, one shows how the growth kinetics imposed by the Cahn-Hilliard equation influences the nucleation process in binary alloys. We find that the classical picture prevails at low supersaturation only, when the size is the unstable variable. When the degree of metastability of the initial phase increases the direction of the nucleation current is modified and the eigenvalue of the nucleation problem is found to be non-monotonic. In terms of nucleation pathways it means that the classical regime is recovered near the binodal limit, the cluster grows with the equilibrium composition. Then an intermediate regime can be seen when supersaturation increases with a concomitant change in size and composition. Moreover, it is found that the clusters properties, as well as nucleation rates, are similar to diffuse-interface theory predictions in the entire metastable region. A more detailed analysis shall be performed to estimate the accuracy of the model, as compared to the diffuse-interface theory of nucleation.

Acknowledgments

The author thanks David Carrière (CEA, NIMBE) and Manon Bonvalet-Rolland (UMET) for fruitful discussions on nucleation theories.

Funding

This work was supported by the ANR TITANS project.

Data availability statement

The data that support the findings of this study are available from the corresponding author upon reasonable request.

References

[1] M. Volmer, *Kinetik der phasenbildung*, Steinkopff, Dresden/Leipzig, 1939.

[2] R. Becker and W. Döring, *Kinetische behandlung der keimbildung in übersättigten dämpfen*, Annalen der Physik 416 (1935), pp. 719–752, Available at https://onlinelibrary.wiley.com/doi/abs/10.1002/andp.19354160806.

[3] J. Zeldovich, *Theory of nucleation and condensation*, Soviet Phys.-JETP 12 (1942), p. 525.

[4] Y. Frenkel, *Kinetic theory of liquids*, Oxford University Press, Oxford, 1946.

[5] D. Turnbull and J.C. Fisher, *Rate of nucleation in condensed systems*, The Journal of Chemical Physics 17 (1949), pp. 71–73, Available at https://doi.org/10.1063/1.1747055.

[6] J. Feder, K.C. Russell, J. Lothe, and G.M. Pound, *Homogeneous nucleation and growth of droplets in vapours*, Advances in Physics 15 (1966), pp. 111–178, Available at https://doi.org/10.1080/00018736600101264.

[7] D. Reguera and H. Reiss, *Nucleation in confined ideal binary mixtures: The renninger–wilemski problem revisited*, The Journal of Chemical Physics 119 (2003), pp. 1533–1546, Available at https://doi.org/10.1063/1.1579685.

[8] A.S. Abyzov and J.W.P. Schmelzer, *Nucleation versus spinodal decomposition in confined binary solutions*, The Journal of Chemical Physics 127 (2007), p. 114504, Available at https://doi.org/10.1063/1.2774989.

[9] S. Prestipino, A. Laio, and E. Tosatti, *Systematic improvement of classical nucleation theory*, Phys. Rev. Lett. 108 (2012), p. 225701, Available at https://link.aps.org/doi/10.1103/PhysRevLett.108.225701.

[10] J. Russo and H. Tanaka, *Crystal nucleation as the ordering of multiple order parameters*, The Journal of Chemical Physics 145 (2016), p. 211801, Available at https://doi.org/10.1063/1.4962166.

[11] W. Lechner, C. Dellago, and P.G. Bolhuis, *Reaction coordinates for the crystal nucleation of colloidal suspensions extracted from the reweighted path ensemble*, The Journal of Chemical Physics 135 (2011), p. 154110, Available at https://doi.org/10.1063/1.3651367.

[12] S. Auer and D. Frenkel, *Prediction of absolute crystal-nucleation rate in hard-sphere colloids*, Nature 409 (2001), pp. 1020–1023, Available at https://doi.org/10.1038/35059035.

[13] J. Russo and H. Tanaka, *The microscopic pathway to crystallization in supercooled liquids*, Scientific Reports 2 (2012), p. 505, Available at https://doi.org/10.1038/srep00505.

[14] Y.iang, G. Díaz Leines, R. Drautz, and J. Rogal, *Identification of a multi-dimensional reaction coordinate for crystal nucleation in Ni3Al*, The Journal of Chemical Physics 152 (2020), p. 224504, Available at https://doi.org/10.1063/5.0010074.

[15] S. Novy, P. Pareige, and C. Pareige, *Atomic scale analysis and phase separation understanding in a thermally aged fe–20at.cr alloy*, Journal of Nuclear Materials 384 (2009), pp. 96–102, Available at https://www.sciencedirect.com/science/article/pii/S0022311508005801.

[16] M. Fine, J. Liu, and M. Asta, *An unsolved mystery: The composition of bcc cu alloy precipitates in bcc fe and steels*, Materials Science and Engineering: A 463 (2007), pp. 271–274, Available at https://www.sciencedirect.com/science/article/pii/S0921509306025640, tMS 2006, Mukherjee Symposium.

[17] J.W. Cahn and J.E. Hilliard, *Free energy of a nonuniform system. iii. nucleation in a two-component incompressible fluid*, The Journal of Chemical Physics 31 (1959), pp. 688–699, Available at https://doi.org/10.1063/1.1730447.

[18] T. Philippe and D. Blavette, *Minimum free-energy pathway of nucleation*, The Journal of Chemical Physics 135 (2011), p. 134508, Available at https://doi.org/10.1063/1.3644935.

[19] T. Philippe, *Nucleation and interfacial adsorption in ternary systems*, The Journal of Chemical Physics 142 (2015), p. 094501, Available at https://doi.org/10.1063/1.4913592.

[20] M. Iwamatsu, *Minimum free-energy path of homogenous nucleation from the phase-field equation*, The Journal of Chemical Physics 130 (2009), p. 244507, Available at https://doi.org/10.1063/1.3158471.

[21] L. Zhang, L.Q. Chen, and Q. Du, *Morphology of critical nuclei in solid-state phase transformations*, Phys. Rev. Lett. 98 (2007), p. 265703, Available at https://link.aps.org/doi/10.1103/PhysRevLett.98.265703.

[22] L. Gránásy, *Diffuse interface theory of nucleation*, Journal of Non-Crystalline Solids 162 (1993), pp. 301 – 303, Available at http://www.sciencedirect.com/science/article/pii/0022309393912507.

[23] Wilhelmsen, D. Bedeaux, S. Kjelstrup, and D. Reguera, *Thermodynamic stability of nanosized multicomponent bubbles/droplets: The square gradient theory and the capillary approach*, The Journal of Chemical Physics 140 (2014), p. 024704, Available at https://doi.org/10.1063/1.4860495.

[24] V. Talanquer and D.W. Oxtoby, *Dynamical density functional theory of gas–liquid nucleation*, The Journal of Chemical Physics 100 (1994), pp. 5190–5200, Available at https://doi.org/10.1063/1.467183.

[25] J.F. Lutsko, *Density functional theory of inhomogeneous liquids. iii. liquid-vapor nucleation*, The Journal of Chemical Physics 129 (2008), p. 244501, Available at https://doi.org/10.1063/1.3043570.

[26] V. Baidakov, G. Boltashev, and J. Schmelzer, *Comparison of different approaches to the determination of the work of critical cluster formation*, Journal of Colloid and Interface Science 231 (2000), pp. 312 – 321, Available at http://www.sciencedirect.com/science/article/pii/S0021979700971480.

[27] J.W.P. Schmelzer, J. Schmelzer, and I.S. Gutzow, *Reconciling gibbs and van der waals: A new approach to nucleation theory*, The Journal of Chemical Physics 112 (2000), pp. 3820–3831, Available at https://doi.org/10.1063/1.481595.

[28] L. Lunéville, P. Garcia, O. Tissot, and D. Simeone, *Non-classical critical precipitates in a nucleation and growth regime: Reconciliation of simulation and experiment*, Applied Physics Letters 121 (2022), p. 184102, Available at https://doi.org/10.1063/5.0122126.

[29] D. Simeone, O. Tissot, P. Garcia, and L. Luneville, *Dynamics of nucleation in solids: A self-consistent phase field approach*, Phys. Rev. Lett. 131 (2023), p. 117101, Available at https://link.aps.org/doi/10.1103/PhysRevLett.131.117101.

[30] H. Reiss and M. Shugard, *On the composition of nuclei in binary systems*, The Journal of Chemical Physics 65 (1976), pp. 5280–5293, Available at https://doi.org/10.1063/1.433028.

[31] T. Philippe and D. Blavette, *Nucleation pathway in coherent precipitation*, Philosophical Magazine 91 (2011), pp. 4606–4622, Available at https://doi.org/10.1080/14786435.2011.616548.

[32] J.W.P. Schmelzer, G.S. Boltachev, and V.G. Baidakov, *Classical and generalized gibbs' approaches and the work of critical cluster formation in nucleation theory*, The Journal of Chemical Physics 124 (2006), p. 194503, Available at https://doi.org/10.1063/1.2196412.

[33] J.W.P. Schmelzer and A.S. Abyzov, *Thermodynamic analysis of nucleation in confined space: Generalized gibbs approach*, The Journal of Chemical Physics 134 (2011), p. 054511, Available at https://doi.org/10.1063/1.3548870.

[34] M. Bonvalet, T. Philippe, X. Sauvage, and D. Blavette, *The influence of size on the composition of nano-precipitates in coherent precipitation*, Philosophical Magazine 94 (2014), pp. 2956–2966, Available at https://doi.org/10.1080/14786435.2014.941029.

[35] J.F. Lutsko and M.A. Durán-Olivencia, *A two-parameter extension of classical nucleation theory*, Journal of Physics: Condensed Matter 27 (2015), p. 235101, Available at https://dx.doi.org/10.1088/0953-8984/27/23/235101.

[36] S. Ghosh and S.K. Ghosh, *Homogeneous nucleation in vapor-liquid phase transition of Lennard-Jones fluids: A density functional theory approach*, The Journal of Chemical Physics 134 (2011), p. 024502, Available at https://doi.org/10.1063/1.3522771.

[37] O. Tissot, P. Gokelaere, P. Garcia, L. Pauchard, C. Pareige, L. Luneville, and D. Simeone, *Reconciliation between simulated and measured microstructures of metastable*

fecr alloys: A phase field approach, Acta Materialia 260 (2023), p. 119303, Available at https://www.sciencedirect.com/science/article/pii/S135964542300633X.

[38] H. Reiss, *The Kinetics of Phase Transitions in Binary Systems*, The Journal of Chemical Physics 18 (1950), pp. 840–848, Available at http://scitation.aip.org/content/aip/journal/jcp/18/6/10.1063/1.1747784.

[39] D. Stauffer, *Kinetic theory of two-component ("hetero-molecular") nucleation and condensation*, Journal of Aerosol Science 7 (1976), pp. 319–333, Available at http://www.sciencedirect.com/science/article/pii/0021850276900860.

[40] G. Wilemski, *Binary nucleation kinetics. IV. Directional properties and cluster concentrations at the saddle point*, The Journal of Chemical Physics 110 (1999), pp. 6451–6457, Available at https://aip.scitation.org/doi/abs/10.1063/1.478547.

[41] H. Trinkaus, *Theory of the nucleation of multicomponent precipitates*, Physical Review B 27 (1983), pp. 7372–7378, Available at https://link.aps.org/doi/10.1103/PhysRevB.27.7372.

[42] B.E. Wyslouzil and G. Wilemski, *Binary nucleation kinetics. II. Numerical solution of the birth–death equations*, The Journal of Chemical Physics 103 (1995), pp. 1137–1151, Available at https://aip.scitation.org/doi/abs/10.1063/1.469824.

[43] B.E. Wyslouzil and G. Wilemski, *Binary nucleation kinetics. III. Transient behavior and time lags*, The Journal of Chemical Physics 105 (1996), pp. 1090–1100, Available at https://aip.scitation.org/doi/abs/10.1063/1.471953.

[44] S.P. Fisenko and G. Wilemski, *Kinetics of binary nucleation of vapors in size and composition space*, Physical Review. E, Statistical, Nonlinear, and Soft Matter Physics 70 (2004), p. 056119.

[45] N.V. Alekseechkin, *Multivariable kinetic theory of the first order phase transitions*, The Journal of Chemical Physics 124 (2006), p. 124512, Available at http://scitation.aip.org/content/aip/journal/jcp/124/12/10.1063/1.2178781.

[46] J.F. Lutsko, *Communication: A dynamical theory of homogeneous nucleation for colloids and macromolecules*, The Journal of Chemical Physics 135 (2011), p. 161101, Available at https://doi.org/10.1063/1.3657400.

[47] J.F. Lutsko, *A dynamical theory of nucleation for colloids and macromolecules*, The Journal of Chemical Physics 136 (2012), p. 034509, Available at https://doi.org/10.1063/1.3677191.

[48] E.M. Lifshits and L.P. Pitaevskii, *Physical kinetics /*, Course of theoretical physics ;, Pergamon Press,, Oxford :, c1981.

[49] V.A. Shneidman, *Transient nucleation with a monotonically changing barrier*, Phys. Rev. E 82 (2010), p. 031603, Available at https://link.aps.org/doi/10.1103/PhysRevE.82.031603.

[50] E.V. Makoveeva, D.V. Alexandrov, A.A. Ivanov, and I.V. Alexandrova, *Desupersaturation dynamics in solutions with applications to bovine and porcine insulin crystallization*, Journal of Physics A: Mathematical and Theoretical 56 (2023), p. 455702, Available at https://dx.doi.org/10.1088/1751-8121/ad0202.

[51] D.V. Alexandrov and A.P. Malygin, *Nucleation kinetics and crystal growth with fluc-*

tuating rates at the intermediate stage of phase transitions, Modelling and Simulation in Materials Science and Engineering 22 (2013), p. 015003, Available at https://dx.doi.org/10.1088/0965-0393/22/1/015003.

[52] T. Philippe, M. Bonvalet, and D. Blavette, *Kinetic theory of diffusion-limited nucleation*, The Journal of Chemical Physics 144 (2016), p. 204501, Available at http://aip.scitation.org/doi/abs/10.1063/1.4950878.

[53] Y. Buyevich and V. Mansurov, *Kinetics of the intermediate stage of phase transition in batch crystallization*, Journal of Crystal Growth 104 (1990), pp. 861–867, Available at https://www.sciencedirect.com/science/article/pii/002202489090112X.

[54] D. Barlow, *Theory of the intermediate stage of crystal growth with applications to protein crystallization*, Journal of Crystal Growth 311 (2009), pp. 2480–2483, Available at https://www.sciencedirect.com/science/article/pii/S0022024809002723.

[55] D. Barlow, *Theory of the intermediate stage of crystal growth with applications to insulin crystallization*, Journal of Crystal Growth 470 (2017), pp. 8–14, Available at https://www.sciencedirect.com/science/article/pii/S002202481730221X.

[56] J. Langer, *Statistical theory of the decay of metastable states*, Annals of Physics 54 (1969), pp. 258–275, Available at https://www.sciencedirect.com/science/article/pii/0003491669901535.

[57] J.S. Langer and L.A. Turski, *Hydrodynamic model of the condensation of a vapor near its critical point*, Phys. Rev. A 8 (1973), pp. 3230–3243, Available at https://link.aps.org/doi/10.1103/PhysRevA.8.3230.

[58] J.F. Lutsko, *Systematically extending classical nucleation theory*, New Journal of Physics 20 (2018), p. 103015, Available at https://dx.doi.org/10.1088/1367-2630/aae174.

[59] M.A. Durán-Olivencia, P. Yatsyshin, S. Kalliadasis, and J.F. Lutsko, *General framework for nonclassical nucleation*, New Journal of Physics 20 (2018), p. 083019, Available at https://dx.doi.org/10.1088/1367-2630/aad170.

[60] O. Tissot, C. Pareige, M.H. Mathon, M. Roussel, E. Meslin, B. Décamps, and J. Henry, *Comparison between sans and apt measurements in a thermally aged fe-19at.cr alloy*, Materials Characterization 151 (2019), pp. 332–341, Available at https://www.sciencedirect.com/science/article/pii/S1044580318330511.

[61] W. Xiong, P. Hedström, M. Selleby, J. Odqvist, M. Thuvander, and Q. Chen, *An improved thermodynamic modeling of the fe–cr system down to zero kelvin coupled with key experiments*, Calphad 35 (2011), pp. 355–366, Available at https://www.sciencedirect.com/science/article/pii/S0364591611000460.

[62] A. Jacob, E. Povoden-Karadeniz, and E. Kozeschnik, *Revised thermodynamic description of the fe-cr system based on an improved sublattice model of the phase*, Calphad 60 (2018), pp. 16–28, Available at https://www.sciencedirect.com/science/article/pii/S0364591617301116.

[63] C. Pareige, M. Roussel, S. Novy, V. Kuksenko, P. Olsson, C. Domain, and P. Pareige, *Kinetic study of phase transformation in a highly concentrated fe–cr alloy: Monte carlo simulation versus experiments*, Acta Materialia 59 (2011), pp. 2404–2411,

Available at https://www.sciencedirect.com/science/article/pii/S1359645410008700.
[64] E. Martínez, O. Senninger, C.C. Fu, and F. Soisson, *Decomposition kinetics of fe-cr solid solutions during thermal aging*, Phys. Rev. B 86 (2012), p. 224109, Available at https://link.aps.org/doi/10.1103/PhysRevB.86.224109.